Rhodium(III) Cage Compounds Based on Diphenylglycoluril

Frank G. M. Niele,[†] Constantinus F. Martens,[†] and Roeland J. M. Nolte*[,‡]

Contribution from the Department of Organic Chemistry, University of Utrecht, 3584 CH Utrecht, The Netherlands, and the Department of Organic Chemistry, University of Nijmegen, 6525 ED Nijmegen, The Netherlands. *Received May 2, 1988*

Abstract: Metallo hosts containing an intramolecular cavity as well as a potentially active rhodium center have been synthesized from the concave building block tetrahydro-3a,6a-diphenylimidazo[4,5-*d*]imidazole-2,5(1*H*,3*H*)-dione (diphenylglycoluril, BB1) and its 1,3:4,6-bis(1,4-dihydroxy-2,3-xylylene) derivative (BB2). To this end the ureylene nitrogen atoms of BB1 and the hydroxyl oxygen atoms of BB2 are provided with arms A, which are furnished with potential substrate binding sites and terminated with metal-binding groups X: BB-$(A-X)_4$, A = ethylene glycol ether chain, X = 1-imidazolyl (Im), 1-benzimidazolyl (Benz), or 3-pyridyl (Py). Reaction of BB1-$(A-X)_4$ (A = $CH_2(OCH_2CH_2)_n$ (n = 1 and 2), X = Im) with $RhCl_3 \cdot 3H_2O$ results in the formation of complexes with general formula *trans*-[Rh(BB1-$(A-X)_4)Cl_2$]Cl. These complexes have a cage structure with four imidazolyl groups in one plane with the rhodium center and two Cl ligands coordinated perpendicular to this plane. One of the *trans*-chloro atoms is located inside the cavity. When in BB1-$(A-X)_4$, the arm A = $CH_2(OCH_2CH_2)_3$, a cis complex is formed with Rh(III). The corresponding benzimidazole complex (A = $CH_2(OCH_2CH_2)_3$, X = Benz), however, has the trans configuration. The origin of these different configurations is discussed. Complexes prepared from BB2-$(A-X)_4$ (A = $CH_2CH_2(OCH_2CH_2)_n$ (n = 1 and 2), X = Benz and A = $(CH_2CH_2O)_2CH_2$, X = Py) and Rh(III) all have the trans configuration.

There is currently great interest in the important and very promising field of intramolecular inclusion chemistry.[1] A principal theme in this field is the molecular design of inclusion catalysts that mimics nature's unsurpassed enzymes.[2] When one realizes the great importance of metals in biocatalysis[3] as well as current artificial catalysis,[4] it is surprising to find that the development of "metallo inclusion catalysts" has lagged behind that of their organic counterparts. Besides some incidental examples,[5] Busch, Mansuy, and Suslick have presented interesting studies that combine a metal ion's catalytic power and a cavity-containing molecule's ability to select and orient a substrate.[6,7]

An inclusion catalyst should contain binding and catalytic sites that converge on an enclosed guest molecule. Rebek concluded that the topology of most organic, cavity-containing hosts (cyclodextrins, crown ethers, and cyclophanes) do not fulfill this requirement because functional groups attached to the outer surface of these hosts point away from the enclosed substrates (see Figure 1, left).[8]

In this paper we describe the design, synthesis, and characterization of new macropolycyclic metallo cages containing relatively large cavities with a potentially active rhodium(III) center adjacent to a substrate binding site (see Figure 1, right). The metallo cages are based on the concave building block diphenylglycoluril, which was previously described by us.[6] In addition, two new types of heterotopic tetrapodal ligands (tetrapodands), based on the novel concave building block **5**, are presented.[9] It will be demonstrated that our tetrapodands can introduce unexpected "macroligand effects".

Results and Discussion

Molecular Design. In a previous paper[6] we introduced the metallo cage strategy for the preparation of a macropolycyclic metallo host: to a concave building block (BB) are attached four spacer units (A), comprising chains furnished with potential substrate binding sites, terminated with metal-binding groups (L) to yield a so-called tetrapodand; subsequent coordination of the four ligating groups (L) to a metal center (M) results in the creation of a metallo cage (see Figure 2). In the present paper we extend the metallo cage strategy as follows. It is intended to bind the four ligating groups of one tetrapodand kinetically inert in one plane (xy plane) with the metal center, while other more weakly coordinated ligands, which can be substituted more easily, are present along the axis perpendicular to this plane.

We have used diphenylglycoluril (BB1, **1**; see Chart I)[6] and 1,3:4,6-bis(1,4-dihydroxy-2,3-xylylene)tetrahydro-3a,6a-diphenylimidazo[4,5-*d*]imidazole-2,5(1*H*,3*H*)-dione (BB2, **5**) as basic building blocks in our study. The latter is more concave

Chart I

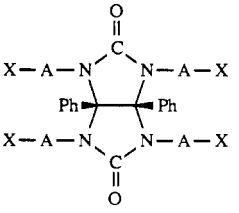

Short-hand notation: BB1-$(A-X)_4$

1: A = H
2a: A = $CH_2(OCH_2CH_2)_2$, X = Im (=1-imidazolyl)
2b: A = $CH_2OCH_2CH_2$, X = Im
3: A = $CH_2(OCH_2CH_2)_3$, X = Im
4: A = $CH_2(OCH_2CH_2)_3$, X = Benz (=1-benzimidazolyl)

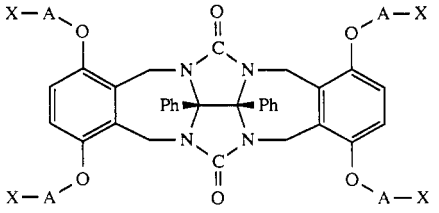

Short-hand notation: BB2-$(A-X)_4$

5: A = H
6a: A = $CH_2CH_2OCH_2CH_2$, X = Cl
6b: A = $CH_2CH_2OCH_2CH_2$, X = Benz
7a: A = $CH_2CH_2(OCH_2CH_2)_2$, X = Cl
7b: A = $CH_2CH_2(OCH_2CH_2)_2$, X = Benz
8: A = $(CH_2)_3$, X = Py (=3-pyridyl)
9: A = $CH_2CH_2OCH_2CH_2OCH_2$, X = Py

[†] University of Utrecht.
[‡] University of Nijmegen.

(1) (a) Lehn, J. M. *Science* **1985**, *227*, 849-856. (b) Hamilton, A.; Lehn, J.-M.; Sestler, J. L. *J. Am. Chem. Soc.* **1986**, *108*, 5158-5167. (c) Tsuchida, E.; Nishide, H. *Top. Curr. Chem.* **1986**, *132*, 63-99. (d) Franke, J.; Vögtle, F. *Ibid.* 135-170.

(2) (a) Cramer, F. *Chem. Ber.* **1953**, *86*, 1576-1581. (b) Breslow, R.; Campbell, P. *J. Am. Chem. Soc.* **1969**, *91*, 3085. (c) Chao, Y.; Cram, D. J. *J. Am. Chem. Soc.* **1976**, *98*, 1015-1017. (d) Murakami, Y. *Top Curr. Chem.* **1983**, *115*, 107-155. (e) Schmidtchen, F. P. *Ibid.* **1986**, *132*, 101-133. (f) D'Souza, V. T.; Bender, M. L. *Acc. Chem. Res.* **1987**, *20*, 146-152.

(3) (a) Ibers, J. A.; Holm, R. H. *Science* **1980**, *209*, 223-235. (b) Dugas, H.; Penney, C. *Bioorganic Chemistry, A Chemical Approach to Enzyme Action*; Springer-Verlag: New York, 1981.

(4) (a) Boubart, M. *J. Mol. Catal., Review Issue* **1986**, 29-41. (b) Waller, F. J. *Ibid.* 43-61.

0002-7863/89/1511-2078$01.50/0

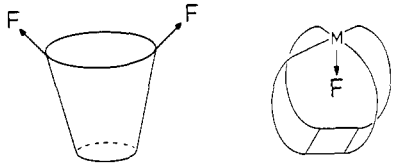

Figure 1. (Left) Divergent functional groups (F) on cavity-containing molecules such as cyclodextrins, crown ethers, and cyclophanes. (Right) A convergent functionality F pointing toward the substrate binding site of a metallo cage.

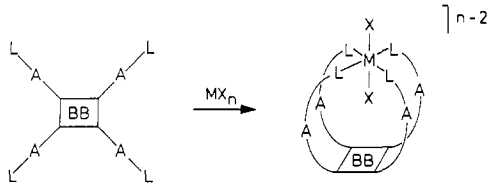

Figure 2. Metallo cage strategy.

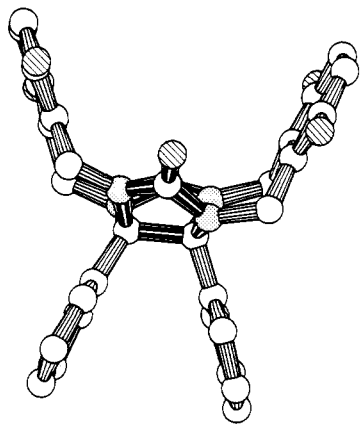

Figure 3. X-ray structure of basic building block BB2-H_4 (**5**).

and more preorganized[10] than the former as it contains two *o*-xylylene side walls (see Figure 3).[9] The spacer units attached to **1** and **5** consist of ethylene glycol ether chains or of a short trimethylene chain.

We have chosen Rh(III) as a metal center, because it is known to form kinetically stable octahedral complexes of the type *trans*-[RhL_4X_2]X (wherein L is an N-donating ligand, e.g. pyridine, pyrimidine, or thiazole, and X is a halogen).[11] These complexes perfectly meet the requirements of the above formulated metallo cage strategy.

As a ligating group we have at first chosen imidazole. This aromatic heterocyclic five-membered ring contains a pyrrole-like nitrogen (N1), which can easily be alkylated (for attachment of a spacer), and a pyridine-like nitrogen (N3), which is able to stabilize various metal ions.[3a] In this context it is of interest to mention that complexes of Rh(III) and 1-methylimidazole are almost as stable as their amine analogues.[11] The robustness of the latter complexes ensures that photochemical reactions can be studied even under ambient conditions without interference from thermal reactions.[12] For strategic reasons (vide infra) we later on switched over to the imidazole derivative benzimidazole.

A pyridyl unit provides the third ligating group. First, one reason for this choice is that with this ligand complexes of the type *trans*-[RhL_4X_2]X, wherein L is a substituted pyridine, are easily accessible.[11] Second, the (substitution) chemistry of rhodium(III)–pyridyl complexes has been studied relatively well. For instance, an interesting property of *trans*-[$Rh(pyr)_4Cl_2$]$^+$ (pyr = pyridine) is the possibility to form, by reaction with BH_4^-, the cationic *trans*-[Rh(pyridine)$_4$ClH]$^+$,[13] a species that is supposed to act as a hydride-transfer agent. A metallo cage with a *trans*-[$Rh(pyridine)_4Cl_2$]$^+$ "roof" could, therefore, open up a new way to reduce a bound substrate regioselectively. The 3-position of the pyridine ring has been selected for the attachment of the spacer unit. The reason for this is architectural; CPK models demonstrate that position 3 is the most suitable one for building a cavity-containing metallo cage. Attachment via position 4 forces the groups to bend outward, and the 2-position is not suitable for steric reasons.

Tetrapodands. The tetrapodands **2b**, **3**, and **4** were synthesized in a way similar to that reported previously for tetrapodand **2a** (see also the Experimental Part).[6]

The reaction path for the tetrapodands **6b** and **7b** is outlined in Scheme I. Synthesis starts with the reaction of BB2-H_4 (**5**) with an ω-chlorotosylate. At room temperature, with DMSO as a solvent and solid KOH as a base, selective alkylation takes place with tosylate acting as a leaving group, yielding the tetrachlorides **6a** and **7a**. Subsequently, an in situ prepared benzimidazolate nucleophile can be substituted for a chloride yielding the tetrapodands **6b** and **7b**. An advantage of this method over the one with a dichloride or ditosylate is that intra-[9] and intermolecular bridge forming between the BB2-H_4 hydroxy oxygens is prevented.

Scheme II shows the route to the tetra(3-pyridyl) podands. The first one, **8**, has a trimethylene spacer; it is prepared by reacting building block **5** with the bromide **10**·HBr. The second one, **9**, has two CH_2OCH_2 groups in each spacer unit. Its preparation starts with the reaction of 3-pyridylmethanol with 5-tosyl-1-

Scheme I

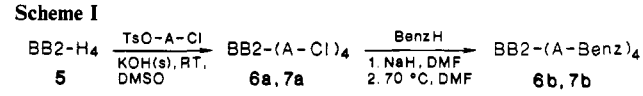

Scheme II

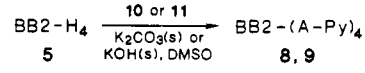

Table I. Gel Permeation Results[a]

tetrapodand	elution time, min: free tetrapodand	elution time, min: corresponding Rh cage
2a	27.5	25.6
2b	28.6	26.0
3	26.3	27.4
4	27.0	28.8
6b	30.8	31.5
7b	29.3	31.4
8	29.9	30.3
9	27.2	28.9

[a] Sephadex LH-60 column; see the Experimental Part.

(5) (a) Breslow, R.; Overman, L. E. *J. Am. Chem. Soc.* **1970**, *92*, 1075–1077. (b) Tabushi, I.; Kuroda, Y.; Mochizuki, A. *J. Am. Chem. Soc.* **1980**, *102*, 1152–1153. (c) Groves, J. T.; Myers, R. S. *J. Am. Chem. Soc.* **1983**, *105*, 5791–5796.

(6) Niele, F. G. M.; Nolte, R. J. M. *J. Am. Chem. Soc.* **1988**, *110*, 172–177.

(7) (a) Alcock, N. W.; Lin, W.-K.; Jircitano, A.; Mokren, J. D.; Corfield, P. W. R.; Johnson, G.; Novotnak, G.; Cairns, C.; Busch, D. H. *Inorg. Chem.* **1987**, *26*, 440–452, and references therein. (b) Mansuy, D.; Battioni, J.-P.; Renaud, J. P.; Guerin, P. *J. Chem. Soc., Chem. Commun.* **1985**, 155–156. (c) Mansuy, D. *Pure Appl. Chem.* **1987**, *59*, 766–767. (d) Cook, B. R.; Reinert, T. J.; Suslick, K. S. *J. Am. Chem. Soc.* **1986**, *108*, 7281–7286. (e) Suslick, K. S.; Cook, B. R. *J. Chem. Soc., Chem. Commun.* **1987**, 200–202.

(8) (a) Rebek, J., Jr.; Askew, B.; Killoran, M.; Nemeth, D.; Lin, F.-T. *J. Am. Chem. Soc.* **1987**, *109*, 2426–2431. (b) Rebek, J., Jr. *Science* **1987**, *235*, 1478–1484.

(9) Smeets, J. W. H.; Sijbesma, R. P.; Niele, F. G. M.; Spek, A. L.; Smeets, W. J. J.; Nolte, R. J. M. *J. Am. Chem. Soc.* **1987**, *109*, 928.

(10) For a discussion about the principle of preorganization, see: Doxsee, K. M.; Feigel, M.; Stewart, K. D.; Canary, J. W.; Knobler, C. B.; Cram, D. J. *J. Am. Chem. Soc.* **1987**, *109*, 3098–3107, and references therein.

(11) Addison, A. W.; Dawson, K.; Gillard, R. D.; Heaton, B. T.; Shaw, H. *J. Chem. Soc., Dalton Trans.* **1972**, 589–596.

(12) Skebsted, L. H. *Coord. Chem. Rev.* **1985**, *64*, 343–359.

(13) (a) Gillard, R. D.; Wilkinson, G. *J. Chem. Soc.* **1963**, 3594–3599. (b) Osborn, J. A.; Gillard, R. D.; Wilkinson, G. *J. Chem. Soc.* **1964**, 3168–3173.

Table II. Molar Conductivities[a] and d–d Transitions of Rhodium Complexes in Methanol

compd	Λ_m, Ω^{-1} cm^2 mol^{-1}	λ_{max}(d–d), nm
trans-[Rh(**2a**)Cl_2]Cl	105	*b*
trans-[Rh(**2b**)Cl_2]Cl	106	*b*
ex-cis-[Rh(**3**)Cl_2]Cl	140	*b*
trans-[Rh(**4**)Cl_2]Cl	108	419
trans-[Rh(**6b**)Cl_2]Cl	104	415
	44[c]	414[c]
	33[d]	410[d]
trans-[Rh(**7b**)Cl_2]Cl	100	416
trans-[Rh(**8**)Cl_2]Cl	90	*b*
trans-[Rh(**9**)Cl_2]Cl	85	*b*
trans-[Rh(**11**)$_4Cl_2$]Cl	112	411
trans-[Rh(**12**)$_4Cl_2$]Cl	104	418
TEBA[e]	101	

[a] At 25 °C and 10^{-3} M. [b] The d–d transitions are masked by intense bands of the tetrapodands. [c] In DMSO/EtOH (1:1 (v/v)), at 25 °C, 10^{-3} M. [d] In DMSO, at 25 °C, 10^{-3} M. [e] TEBA = triethylbenzylammonium chloride.

chloro-3-oxapentane to give **11**. Thereafter, BB2 (**5**) is alkylated with four molecules of the chloride **11** to afford tetrapodand **9**.

The tetrapodands **2a–11** were characterized by elemental analysis, IR, FABMS, and ^{1}H NMR.

Rhodium(III) Complexes Based on BB1. Reaction of tetrapodand **2a** with $RhCl_3 \cdot 3H_2O$ in methanol as a solvent yields, after workup, a product with a FAB mass spectrum that can be assigned to the ion [Rh(**2a**)Cl_2]$^+$. To make sure that in solution neither oligomeric nor polymeric networks were present, we applied gel permeation chromatography. The results (Table I) clearly show that the product consists of a compound having a molecular size of the same order of magnitude as that of the free tetrapodand, and it can thus be implied that the product is monomeric in solution.

The molar conductivity of the reaction product determined in methanol solution (Table II) is in the range expected for 1:1 electrolytes[14] and agrees with the molecular formula [Rh(**2a**)Cl_2]Cl. Furthermore, the ^{1}H NMR data for this compound (methanol-d_4) indicate that all four imidazolyl groups are coordinated to the rhodium center. Compared to those of the free tetrapodand, the resonances of the NCHN imidazolyl protons in the complex have shifted 0.65 ppm downfield. The appearance of all the imidazolyl protons at exactly the same chemical shift indicates that the imidazolyl groups are symmetrically coordinated to the Rh(III) center in a trans configuration. For a cis configuration, one would expect at least two resonance signals for the NCHN protons (one belonging to a set of ligands trans to a chlorine and another one belonging to a set of mutually trans ligands). The presence of a fast (on the NMR time scale) ligand exchange, for which the two resonances would appear as a single peak, can be excluded since Rh(III) compounds are known to be kinetically inert.[15]

In the proton-decoupled ^{13}C NMR spectrum (methanol-d_4; see Figure 4) the imidazolyl carbon atoms give rise to three sharp signals, indicating again that the four ligands are trans symmetrically bound to the Rh(III) center. Further support for the proposed *trans*-[Rh(**2a**)Cl_2]Cl structure is the similarity of the far-IR spectrum (375–250 cm^{-1}) of our product to that of the complex *trans*-[Rh(1-MeIm)$_4Cl_2$]Cl.[11] A picture of the cage structure of [Rh(**2a**)Cl_2]Cl is given in Figure 5a.

As reported earlier[6] tetrapodand **2a** forms a cage compound with a Pd(II) metal center. We observed that the [Pd(**2a**)]$^{2+}$ cage is unstable and collapses via a twisting motion, most likely as a result of intramolecular H bonding between the polar C(2)H bond of the imidazolyl groups and the CH_2OCH_2 functions in the spacers. The palladium(II) cage alternates between a left- and a right-twisted conformation. A consequence of the cage collapse

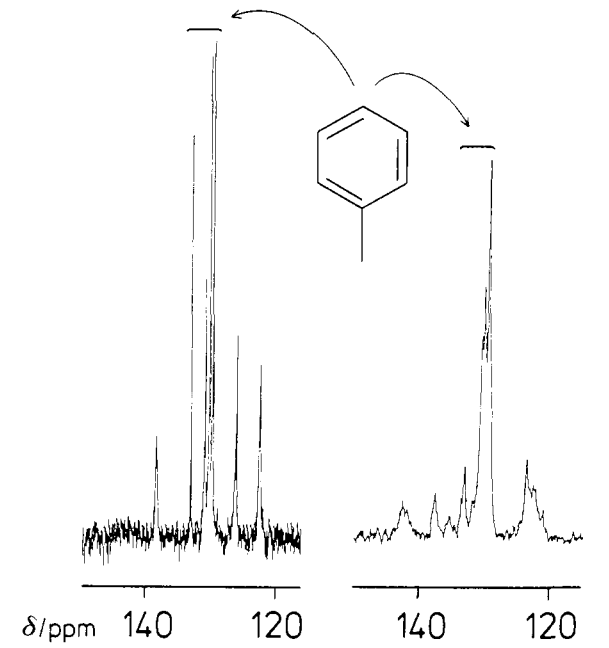

Figure 4. ^{13}C NMR spectra (200 MHz, CD_3OD) in the region 125–135 ppm: (left) *trans*-[Rh(**2a**)Cl_2]Cl, (right) *ex-cis*-[Rh(**3**)Cl_2]Cl. The four peaks belonging to the phenyl carbon atoms are indicated; the other signals originate from the three imidazolyl carbon atoms.

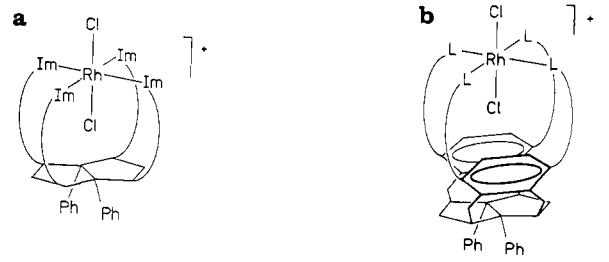

Figure 5. Schematic representation of the metallo cage *trans*-[Rh(**2a**)Cl_2]$^+$ (a). Schematic representation of the metallo cages based on building block BB2 (b).

is that the CH_2Im protons become diastereotopic and possess different chemical shifts.[6] In the ^{1}H NMR spectrum (methanol-d_4) of *trans*-[Rh(**2a**)Cl_2]Cl the resonance pattern of these methylene groups is a normal AA′BB′ pattern. This behavior is what one expects, because in the rhodium complex one of the chloro ligands is inside the cavity, making cage collapse impossible.

Tetrapodand **2b** is equipped with spacers, each of which is one OCH_2CH_2 fragment shorter than those in **2a**. It appears to be difficult to assemble a CPK molecular model of a metallo cage with **2b**, similar to *trans*-[Rh(**2a**)Cl_2]Cl. The reason for this difficulty is that the internal chloro ligand touches the glycoluril unit causing strain in the molecule. The question arises as to whether this monomeric Rh(III) compound can actually be prepared. To find the answer to this question, we carried out the reaction of **2b** with $RhCl_3 \cdot 3H_2O$ in methanol as a solvent. Gel permeation chromatography demonstrates that we are now dealing with a product that is smaller than *trans*-[Rh(**2a**)Cl_2]Cl (see Table I), and it can be concluded that the compound is monomeric. In agreement with this conclusion are the sharp signals present in the ^{1}H NMR spectrum (methanol-d_4). This spectrum shows only one peak for the NCHN imidazolyl protons at 8.1 ppm, i.e. a downfield chemical shift of 0.5 ppm compared to the free tetrapodand. This indicates that the Rh(III) ion is symmetrically surrounded by the imidazolyl ligands in a *trans*-chloro configuration (see above). The molar conductivity of the reaction product determined in methanol solution (Table II) is in the range expected for 1:1 electrolytes.[14] These data confirm that the rhodium complex of tetrapodand **2b**, *trans*-[Rh(**2b**)Cl_2]Cl, can actually be prepared.

(14) Geary, W. J. *Coord. Chem. Rev.* **1971**, *7*, 81–122.
(15) Cotton, F. A.; Wilkinson, G. *Basic Inorganic Chemistry*; Wiley: New York, 1976.

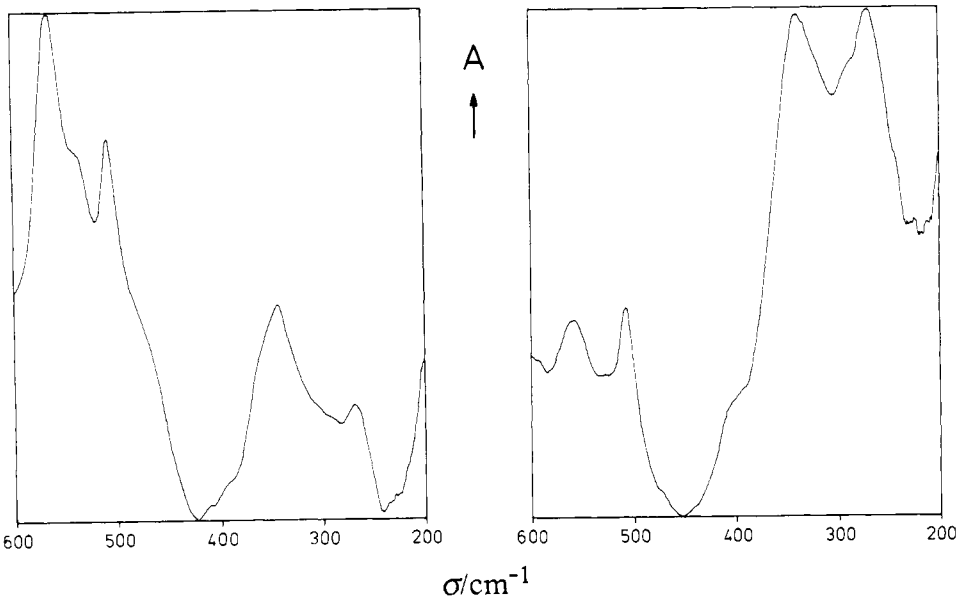

Figure 6. IR spectra in the region 200–600 cm^{-1}: (left) *trans*-[Rh(2a)Cl_2]-Cl; (right) *ex-cis*-[Rh(3)Cl_2]Cl.

The heaviest molecular ion displayed in the FAB mass spectrum of *trans*-[Rh(**2b**)Cl_2]Cl is $(M - 2Cl)^+$ at *m/e* 928. It is remarkable that here the ion $(M - Cl)^+$ is hardly detectable, whereas, for all the other Rh(III) cages presented in this paper, this is the most intense of the Rh-containing molecular ions, all of which are readily identified by virtue of their characteristic isotope patterns. Apparently, the ion *trans*-[Rh(**2b**)Cl_2]$^+$ is more labile than the analogous metallo cages constructed from larger tetrapodands. This is in agreement with the strain observed in the CPK molecular model. Notice that the compound *trans*-[Rh(**2b**)Cl_2]Cl is probably the first *trans*-[RhL_4Cl_2]$^+$ species in which one of the chloro ligands is completely encapsulated and as a consequence is not liable to attack by an incoming ligand.

A consequence of the presence of a chloro ligand inside the cavity is that the cage is largely filled up. To create a bigger cage, we treated tetrapodand **3** with $RhCl_3 \cdot 3H_2O$ under the same conditions as mentioned above for **2a**. However, it is surprising that the spectroscopic data of the isolated rhodium product of **3** are not similar to those of *trans*-[Rh(**2a**)Cl_2]Cl and *trans*-[Rh(**2b**)Cl_2]Cl. One difference is the broadness of the signals in the ^1H NMR spectrum (methanol-d_4) of this new product; this could be due to the presence of various conformations that interconvert on the NMR time scale. However, since raising the temperature to 60 °C did not change the spectrum, such an explanation is unlikely. The origin of the broad signals cannot be the presence of polymeric products, because gel permeation chromatography revealed the complex to be monomeric (Table I). In agreement with this, the FAB mass spectrum showed an isotopic pattern that is attributable to the ion [Rh(**3**)Cl_2]$^+$. The molar conductivity of the product (Table II) lies between that of a 1:1 and a 2:1 electrolyte.[14]

A possible explanation for the deviant behavior of **3** could be that the phenyl groups of the diphenylglycoluril unit fill the cavity. CPK models show this configuration to be possible with tetrapodand **3** but not with the shorter-chained **2a** and **2b**. To check this possibility, we applied ^{13}C NMR spectroscopy. If the cavity is filled, one of the chloro ligands will be positioned close to the two phenyl substituents and the chemical shift of the phenyl carbons will be influenced. The ^{13}C NMR spectrum of the rhodium product of **3** (methanol-d_4) showed the phenyl carbon resonances to have exactly the same chemical shift values as those of the metallo cage *trans*-[Rh(**2a**)Cl_2]Cl (see Figure 4), indicating that the above hypothesis is not correct. We propose that the product derived from **3** has the *cis*-Cl configuration, rather than the *trans*-Cl one. This cis complex has a lower symmetry.

Support for the idea that the rhodium product of **3** has a Rh(III) surrounding different from that of the product of **2a** and **2b** comes from its ^{13}C NMR spectrum, which shows split and broadened signals for the imidazolyl carbon atoms (see Figure 4). Further support comes from the far-IR spectra. Around 350 cm^{-1} (where the rhodium–chloro vibrations are found),[11,16] the spectrum of *trans*-[Rh(**2a**)Cl_2]Cl, while resembling that of *trans*-[Rh(1-MeIm)$_4Cl_2$]Cl, differs significantly from the spectrum of the rhodium product of **3**. In particular, the intensities of the signals in the spectrum of the latter complex (see Figure 6; ν(Rh–Cl) = 360–250 cm^{-1}, ν(Rh–N) = 600–500 cm^{-1}) are consistent with this being a cis complex. Direct comparison, however, with a *cis*-[RhL_4Cl_2]Cl compound (wherein L is an N-alkylated imidazole) is not possible, because such a compound is unknown.

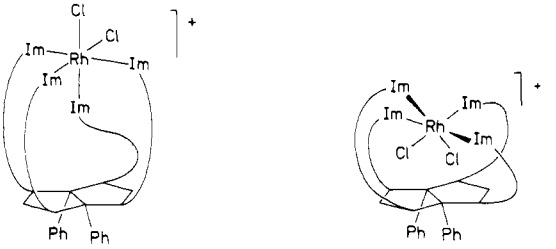

Figure 7. Schematic representations of [Rh(**3**)Cl_2]Cl: (left) the ex-cis configuration, (right) the in-cis configuration.

Two structural isomers having a cis configuration are possible: one in which the two chloro ligands are outside the cavity and one in which these ligands are inside the cavity; we call them the ex-cis and in-cis configurations, respectively (see Figure 7). The CPK model of the in-cis conformer is a strained molecule, whereas, in contrast, the ex-cis conformer is very easy to assemble.

Ligand substitution reactions at Rh(III) centers most likely occur via an associative mechanism.[17,18] Generally, this mechanism involves a transition state in which five ligands nearly remain in their original positions, forming a square pyramid. Two other ligands, the leaving and entering groups, occupy nearly equivalent positions under the base of the square pyramid, at much greater distances from the metal ion than the five former ligands.[17] This transition state accounts for retention of configuration and geometry after a cis nucleophilic attack.[17]

To explain our results, we assume that the reaction intermediate [RhL_3Cl_3]L has the 1,2,4-configuration, consistent with C_{2v} local

(16) Ganguli, J. N.; Bora, T. *Transition Met. Chem.* **1984**, *9*, 88–91.
(17) Johnson, S. A.; Basolo, F.; Pearson, R. G. *J. Am. Chem. Soc.* **1963**, *85*, 1741–1747.
(18) Danny Lo, S. T.; Sisley, M. J.; Swaddly, T. W. *Can. J. Chem.* **1978**, *56*, 2609–2615.

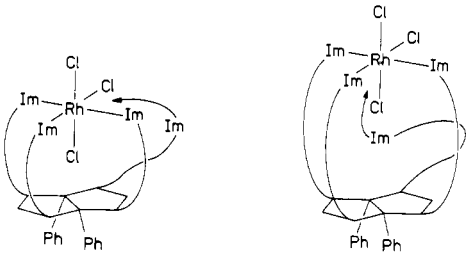

Figure 8. (Left) Screening of the inside chloro ligand in [Rh(**2a**)Cl_3] and attack of an outside one. (Right) Encapsulation of the free imidazolyl ligand in [Rh(**3**)Cl_3] and, consequently, its proper orientation for inside attack.

symmetry. This assumption is in line with literature data, which show that in rhodium(III) complexes with pyridine and various nitriles as N-donating ligands the 1,2,4-isomer appears to be more stable than the 1,2,3-isomer.[19] The origin of the difference in behavior between **2** and **3** is probably due to steric constraints. In the case of tetrapodand **2a** the free arm in $[RhL_3Cl_3]L$ can easily substitute the chloro ligand in the *xy* plane, yielding *trans*-[Rh(**2a**)Cl_2]Cl (see Figure 8, left); the chloro ligand situated in the cavity along the *z* axis is sterically screened by the tetrapodand itself. In addition, the formation of a seven-coordinated transition state in the cavity along the *z* axis is unlikely, because of a lack of space. In the case of tetrapodand **3** the situation is different. The free arm in $[RhL_3Cl_3]L$ can now fill the cavity that has arisen as a result the formation of *ex-cis*-[Rh(**3**)Cl_2]Cl (see Figure 8, right).

Normally, a reaction between $RhCl_3 \cdot 3H_2O$ and an N-donating ligand L yields the trans product $[RhL_4Cl_2]Cl$.[11] It is known, however, that 1-MeIm behaves differently; the reaction of 4 equiv of 1-MeIm with $RhCl_3 \cdot 3H_2O$ in aqueous ethanol always results in the formation of $[Rh(1\text{-MeIm})_5Cl]Cl_2$,[11] and this indicates that an N-alkylated imidazole is able to substitute a chloro ligand along the *z* axis of a Rh(III) center.

In the foregoing discussion it has been explained why attempts to synthesize larger cavities by lengthening the spacer units of the tetrapodand are unsuccessful. To have a better chance of success, we modified our long-chain tetrapodand **3** by substituting benzimidazolyl ligands for the imidazolyl ligands to give tetrapodand **4**. With CPK models the maximum number of benzimidazoles that can be placed around one metal center is four; this limit is imposed by steric factors. CPK models also show that a cis configuration in a complex of type $[M(Benz)_4X_2]X$ is very unlikely.[20]

Prior to this work, no *trans*-$[RhL_4Cl_2]Cl$ compounds in which L is an N-alkylated benzimidazole had been reported. Therefore, we studied the reaction of $RhCl_3 \cdot 3H_2O$ with the model ligand 1-methylbenzimidazole (**12**). With methanol as a solvent, this reaction indeed yielded the required *trans*-[Rh(**12**)$_4Cl_2$]Cl, in quantitative yield. The results of elemental analysis, conductometry, IR, and FABMS are consistent with the proposed molecular formula. The ^1H NMR spectrum ($CDCl_3$) of this model compound showed relatively broad signals. We ascribe this broadness to the following configurational behavior. CPK models suggest a four-bladed propellor-shaped configuration for *trans*-[Rh(**12**)$_4Cl_2$]Cl (see Figure 9). As benzimidazole is asymmetrical, different geometrical configurations are possible depending on the orientation of the *o*-phenylene nucleus. Moreover, in one configuration every proton possesses a site in which its chemical

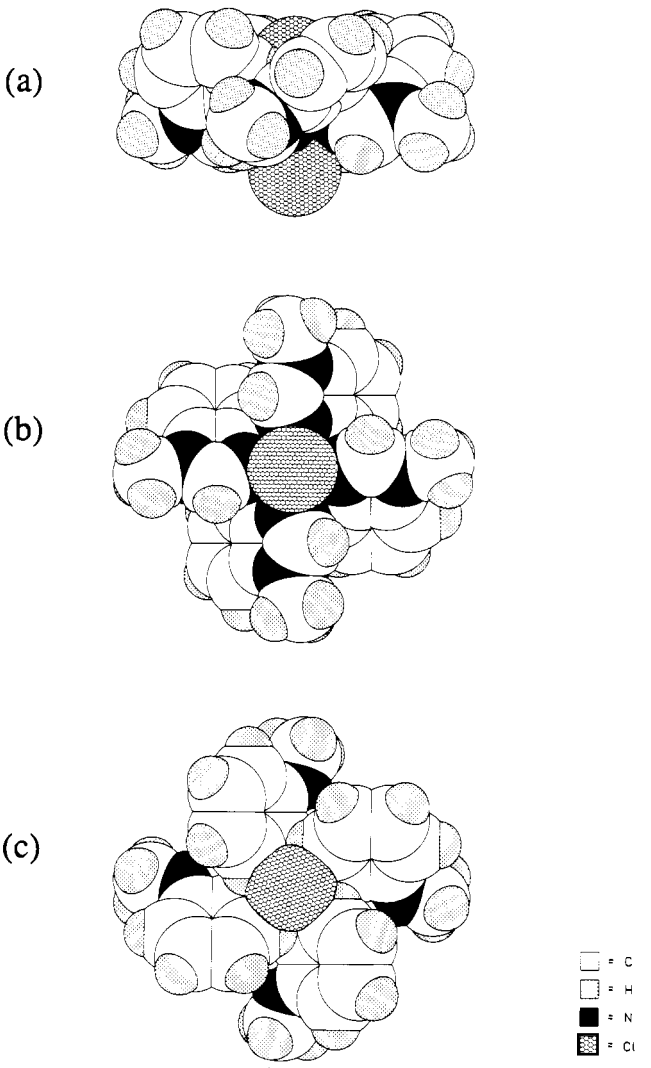

Figure 9. Computer drawings[21] of the propellor-shaped configuration in *trans*-[Rh(**12**)$_4Cl_2$]$^+$. All the *o*-phenylene nuclei are oriented similarly. (a) Side view, reflecting the different steric environments of the chloro ligands. (b) View from below. (c) View from above.

shift is influenced by anisotropy effects induced by neighboring ligands. It is difficult to foresee what kind of isomer distribution will occur. In this context it is worthwhile mentioning that asymmetrically substituted pyridines behave likewise. In particular, in the case of *trans*-$[Ni(3,4\text{-}Me_2pyr)_4](ClO_4)_2$ an X-ray structure determination indicates that a statistical distribution of isomers is present.[16]

The UV–vis spectrum of the model compound showed a d–d transition at 418 nm (methanol), which is characteristic of a *trans*-$[RhL_4Cl_2]Cl$ configuration. For substituted pyridines and imidazoles this transition occurs at 409 ±2 nm.[16] The small red shift observed for *trans*-[Rh(**12**)$_4Cl_2$]Cl might be explained by assuming a tetragonal distortion of the octahedral Rh(III) complex. Presumably, the steric interaction between the *o*-phenylene nucleus and the chloro ligand causes the latter to be pushed away from the Rh(III) center; as a result the ligand field splitting becomes smaller. The presence of these steric interactions is shown in Figure 9.

After having carried out the above-described model reaction, we allowed $RhCl_3 \cdot 3H_2O$ to react with the tetrakis(1-benzimidazolyl) ligand **4** in methanol as a solvent. The product was isolated as a yellow glassy material, which, according to elemental analysis, had the molecular formula Rh(**4**)$Cl_3 \cdot 4H_2O$. The FAB mass spectrum showed a dominant ion with an isotopic pattern fitting the formula $[Rh(4)Cl_2]^+$. In agreement with this finding, the molar conductivity of the complex in methanol (Table II) is in the range for 1:1 electrolytes.[14] Gel permeation chromatography

(19) Gillard, R. D.; Heaton, B. T.; Shaw, H. *Inorg. Chim. Acta* **1972**, *7*, 102–104.
(20) Sundberg, R. J.; Martin, R. B. *Chem. Rev.* **1974**, *74*, 471–517.
(21) For Allinger's molecular mechanics program MM2, see: Allinger, N. L.; Yuh, Y. H. *QCPE* **1981**, *13*, 395. Use of the services and facilities of the Dutch CAOS/CAMM center, under Grants SON-11-20-700 and STW-N-C-H-44,0703, is gratefully acknowledged.
(22) Gillard, R. D.; Heaton, B. T.; Vaughan, D. H. *J. Chem. Soc. A* **1971**, 1840–1846.
(23) Molecular hydrogen is known to catalyze formation of rhodium–pyridine complexes. See: Gillard, R. D.; Osborn, J. A.; Stockwell, P. B.; Wilkinson, G. *Proc. Chem. Soc.* **1964**, 284–285.

demonstrated that the product $[Rh(\mathbf{4})Cl_2]Cl$ is monomeric in solution (Table I).

In the UV–vis spectrum of $[Rh(\mathbf{4})Cl_2]Cl$ the highest wavelength d–d transition is found at 419 nm (Table II). This value is in good agreement with that for the model compound *trans*-$[Rh(\mathbf{12})_4Cl_2]Cl$, indicating that both compounds have a similar octahedral Rh(III) surrounding with trans-sited chloro ligands.

The ^1H NMR spectrum of $[Rh(\mathbf{4})Cl_2]Cl$ ($CDCl_3$) is consistent with the proposed structure. As in *trans*-$[Rh(\mathbf{12})_4Cl_2]Cl$, the benzimidazolyl protons give rise to broad signals and the resonances of the NCHN protons show a downfield chemical shift (of ca. 0.3 ppm relative to the free tetrapodand), which is indicative of a Rh(III)–benzimidazolyl interaction.

A mixture of geometrical isomers, as described above for the complex *trans*-$[Rh(\mathbf{12})_4Cl_2]Cl$, is not likely to occur in the case of *trans*-$[Rh(\mathbf{4})Cl_2]Cl$ since movement of the benzimidazolyl ligands is restricted as a consequence of their connection to the glycoluril building block. CPK models reveal that the configuration with three benzimidazolyl *o*-phenylene units directed outside and one inside the metallo cage contains much strain, especially in the spacer unit of the inside-directed ligand. The complex with all four benzimidazolyl ligands directed outside is by far the easiest one to assemble. In this complex one chloro ligand is situated inside the cage and surrounded by the Rh(III) center and four NCHN benzimidazolyl hydrogen atoms; the other one is situated outside the cage and is surrounded by the Rh(III) center and four *o*-phenylene groups of the benzimidazolyl ligands. Finally, the *trans*-$[Rh(\mathbf{4})Cl_2]Cl$ metallo cage can possess two enantiomeric configurations, a left-handed and a right-handed propellor.

Rhodium(III) Complexes Based on BB2. The reaction between $RhCl_3 \cdot 3H_2O$ and the tetrakis(1-benzimidazolyl) podands **6b** and **7b** yielded the metallo cages *trans*-$[Rh(\mathbf{6b})Cl_2]Cl$ and *trans*-$[Rh(\mathbf{7b})Cl_2]Cl$ (see Figure 5b). According to gel permeation chromatography, the compounds are monomeric (see Table I). The molecular conductivity of the two products is in the range for 1:1 electrolytes (see Table II). In both cases, the FAB mass spectrum displays the molecular ion $(M - Cl)^+$ and the UV–vis spectra are in agreement with a *trans*-$[RhL_4Cl_2]^+$ configuration.

The cage of *trans*-$[Rh(\mathbf{7b})Cl_2]Cl$ is the largest one we have made; in the open conformation it measures about 11 Å from the bottom (the central C–C bond of the glycoluril unit) to the top (the rhodium center). Compared to metallo cages based on building block BB1, the rigid character of building block BB2 makes a collapse of the cage, as occurs in $[Pd(\mathbf{2a})]Cl_2$,[6] impossible.

Before studying the reaction of the tetra(3-pyridyl) podands **8** and **9** with $RhCl_3 \cdot 3H_2O$, we performed a model reaction between $RhCl_3 \cdot 3H_2O$ and 4 equiv of 3-(7-chloro-2,5-dioxaheptyl)pyridine (**11**) in methanol as a solvent. The product of this reaction is a

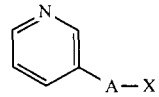

10: A = $(CH_2)_3$, X = Br
11: A = $CH_2(OCH_2CH_2)_2$, X = Cl

yellow compound. Elemental analysis and spectroscopic data are in agreement with a complex of the type *trans*-$[RhL_4Cl_2]Cl$. In particular, the UV–vis spectrum shows a λ_{max}(d–d) that perfectly agrees with the one for *trans*-$[RhL_4Cl_2]Cl$ wherein L is pyridine, 3-ethylpyridine, or 3-aminopyridine.[11] As was mentioned above, tetrakis(pyridine) complexes are known to adopt a four-bladed propellorlike structure.[11] To our knowledge, Rh(III) complexes with cis-coordinated pyridines (viz. *cis*-$[RhPy_4L_2]^+$, $[RhPy_5Cl]^{2+}$, and $[RhPy_6]^{3+}$) have not yet been reported in the literature. In this context Gillard et al. noticed that moderately basic N-donating ligands, such as pyridine, 5-chloro-1-methylimidazole, and 5-nitro-1-methylimidazole, readily give *trans*-$[RhL_4Cl_2]Cl$ whereas more basic ligands such as NH_3 and 1-methylimidazole yield $[RhL_5X]^{2+}$.[11]

Tetrapodand **8** has special features. On the basis of CPK models, its spacer units have the minimum length required to build a metallo cage. This metallo cage is very rigid and as a result well-defined. The model reveals that a cis configuration is not possible. Interestingly, the CPK model predicts a loss of C_2 symmetry of the metallo cage: the propellorlike geometry forces the $[RhL_4Cl_2]^+$ moiety to adopt a conformation in which the Cl–Rh–Cl axis no longer coincides with the molecular axis of the building block BB2. As a consequence of this asymmetry the ^1H NMR spectrum should display broadened signals. Reaction of $RhCl_3 \cdot 3H_2O$ with tetrapodand **8** in methanol as a solvent yields a product that was characterized as $[Rh(\mathbf{8})Cl_2]Cl$ (see Tables I and II and the Experimental Part). It was not possible to detect the λ_{max}(d–d) transition in the UV–vis spectrum, because it was masked by podand bands. As expected, the ^1H NMR spectrum ($CDCl_3$) indeed showed broad signals, with one exception: the phenyl proton resonances at approximately 7 ppm had not broadened upon complexation; they are situated outside the metallo cage and do not "feel" the asymmetry introduced by the Rh(III) complexation.

Finally, we performed a reaction between $RhCl_3 \cdot 3H_2O$ and the tetra(3-pyridyl) podand **9**. The yellow product was characterized (see Tables I and II and the Experimental Part) as $[Rh(\mathbf{9})Cl_2]Cl$. This compound has a relatively large cavity with most likely a *trans*-$[Rh(Py)_4Cl_2]^+$ moiety as roof.

Monomer versus Polymer. It may be asked why monomeric instead of polymeric complexes are formed with the ligands we have used. Since the arms of our tetrapodands are relatively long the enthalpy of complexation to the metal will be similar for monomer and polymer. Thus, the entropy terms will be predominant. Accordingly, since the polymer, being a three-dimensional network with low flexibility, would have an entropy appreciably lower than that of the monomer, formation of the monomer will be preferred.

As Pd(II) forms kinetically labile complexes, the thermodynamically more stable monomer will be obtained.[6] In contrast, complexes of the type $[RhL_4Cl_2]Cl$ are kinetically inert. This means that any kinetically formed polymer would not simply give monomers. The reason we obtain monomeric cages in good yields could be that the intermediate preceding cage formation, viz. $[RhL_3Cl_3]L$, is kinetically labile.

Conclusion

Several cavity-containing Rh(III) compounds have been prepared and characterized. Unexpected from the point of view of "normal" coordination chemistry is the formation of the *ex-cis*-Rh(III) complex using the long-chain tetra(1-imidazolyl) podand **3**, whereas the similar podands **2a** and **2b**, having shorter spacers, yield *trans*-$[RhL_4Cl_2]Cl$ species. Tetrapodands in which the arms are terminated with 1-benzimidazolyl or 3-pyridyl ligating groups give the *trans*-$[RhL_4Cl_2]Cl$ complexes exclusively.

Experimental Part

General Procedures. ^1H NMR spectra were recorded on Varian EM-360, Bruker AW-80, and Bruker WP-200 instruments. Chemical shifts (δ) are reported downfield from internal $(CH_3)_4Si$. Abbreviations used are s = singlet, d = doublet, t = triplet, q = quartet, m = multiplet, and br = broad. Infrared and UV–vis spectra were taken on Perkin-Elmer 283 and Perkin-Elmer 555 spectrophotometers, respectively. The far-IR data were measured via the transreflection method using a Perkin-Elmer 1710 interferometer. FAB mass spectra were recorded on a VG ZAB 2F spectrometer (matrix: glycerol, thioglycerol, *m*-nitrobenzyl alcohol). Conductivity measurements were carried out at 25.0 °C on a Philips PW 9501 conductivity meter. Elemental analyses were carried out by the Elemental Analytical Section of the Institute for Applied Chemistry TNO Zeist, The Netherlands. Melting points were determined on a Mettler FP5/FP51 photoelectric melting point apparatus. Gel permeation chromatography was performed on a Sephadex LH-60 column (length 22 cm, diameter 1 cm) with methanol as eluent at a flow rate of 31 mL/h.

Unless otherwise indicated, commercial chemicals were used as received. DMSO, DMF, and methanol were dried over 3-Å sieves prior to use. Diethyl ether and chloroform were distilled from benzophenone ketyl and $CaCl_2$, respectively.

Compounds. Tetrahydro-3a,6a-diphenylimidazo[4,5-*d*]imidazole-2,5-(1*H*,3*H*)-dione (1). This compound was synthesized according to a literature procedure.[24]

1,3,4,6-Tetrakis(7-(1-imidazolyl)-2,5-dioxaheptyl)tetrahydro-3a,6a-diphenylimidazo[4,5-*d*]imidazole-2,5(1*H*,3*H*)-dione (2a). The synthesis of this compound has been published previously.[6]

1,3,4,6-Tetrakis(4-(1-imidazolyl)-2-oxabutyl)tetrahydro-3a,6a-diphenylimidazo[4,5-*d*]imidazole-2,5(1*H*,3*H*)-dione (2b). The synthesis of this compound has been published previously.[6]

1,3,4,6-Tetrakis(10-(1-imidazolyl)-2,5,8-trioxadecyl)tetrahydro-3a,6a-diphenylimidazo[4,5-*d*]imidazole-2,5(1*H*,3*H*)-dione (3). This compound was prepared as described for **2a** using 1-chloro-8-hydroxy-3,6-dioxaoctane instead of 1-chloro-5-hydroxy-3-oxapentane.[6] The resulting tetrachloride is a light yellow syrup. Conversion with sodium imidazolate yields **3**, which was purified on Sephadex LH 60, using methanol as eluent. Compound **3** was obtained as a light yellow syrup: yield 56%; FABMS $(M + H)^+$ *m/e* 1143; IR (NaCl disks) 1730 (C=O), 1130–1000 (COC) cm^{-1}; ^1H NMR ($CDCl_3$) δ 7.67 (pseudo s, 4 H, NCHN), 7.18 (dd, $^3J \cong {}^4J$ = 1.5 Hz, 4 H, N(1)C*H*CHN(3)), 7.0–6.8 (m, 14 H, ArH and N(1)CHC*H*N(3)), 4.8 (AB q, J_{gem} = 12 Hz, 8 H, NCH_2O), 4.2 (pseudo t, 8 H, CH_2Im), 3.7–3.1 (m, 40 H, $(OCH_2CH_2)_2OCH_2$). Anal. Calcd for $C_{56}H_{78}N_{12}O_{14}\cdot(H_2O)_{4.5}$: C, 54.88; H, 7.12; N, 13.72; O, 24.17. Found: C, 54.78; H, 7.22; N, 13.99; O, 23.75.

1,3,4,6-Tetrakis(10-(1-benzimidazolyl)-2,5,8-trioxadecyl)tetrahydro-3a,6a-diphenylimidazo[4,5-*d*]imidazole-2,5(1*H*,3*H*)-dione (4). The synthetic procedure for **4** is the same as described for **3**. The workup is as follows. After reaction the resulting mixture was treated with 0.2 mL of water and evaporated under water vapor pressure (65 °C). The residue was dissolved in 20 mL of $CHCl_3$ and washed (10×) with 15 mL of weakly acidic water (the pH was adjusted to 6 with concentrated HCl), dried ($MgSO_4$), and evaporated in vacuo: yield approximately 85% of **4** as a light yellow syrup; FABMS $(M + H)^+$ *m/e* 1343; ^1H NMR ($CDCl_3$) δ 7.9–7.1 (m, br, 20 H, benzimidazole), remaining signals as for **3**. Anal. Calcd for $C_{72}H_{86}N_{12}O_{14}\cdot(H_2O)_{2.4}$: C, 62.31; H, 6.55; N, 12.11; O, 18.92. Found: C, 62.40; H, 6.79; N, 11.56; O, 18.60.

1,3:4,6-Bis(1,4-dihydroxy-2,3-xylylene)tetrahydro-3a,6a-diphenylimidazo[4,5-*d*]imidazole-2,5(1*H*,3*H*)-dione (5). This compound was synthesized as described in literature.[9]

1,3:4,6-Bis(1,4-(6-chloro-1,4-dioxahexyl)-2,3-xylylene)tetrahydro-3a,6a-diphenylimidazo[4,5-*d*]imidazole-2,5(1*H*,3*H*)-dione (6a). Under a nitrogen atmosphere compound **5** (2.81 g, 5 mmol) was dissolved in 56.2 mL of DMSO containing 11.2 g of powdered KOH. After the solution was stirred at room temperature for 1 h, 1-tosyl-5-chloro-3-oxapentane (8.57 g, 30 mmol) was added. This mixture was stirred at room temperature for 10 h and thereafter added dropwise, while stirring vigorously, to a mixture of 400 mL of doubly distilled water and 50 mL of diethyl ether. The pH of the solution was kept between 5 and 7 by adding concentrated HCl. The precipitate was filtered, washed with water and diethyl ether (10×), and dried in vacuo: yield 3.6 g (74%) of **6a** as a white solid; mp >210 °C (dec); IR (KBr) 1720 (C=O), 1130–1070 (COC), 735 (CCl) cm^{-1}; ^1H NMR ($CDCl_3$) δ 6.9 (s, 10 H, PhH), 6.5 (s, 4 H, XyH), 5.4 (d from AB q, 4 H, NC*H*H), 3.8 (m, 36 H, NCH*H* and $OCH_2CH_2OCH_2CH_2Cl$). Compound **6a** was converted into **6b** without further purification.

1,3:4,6-Bis[1,4-(6-(1-benzimidazolyl)-1,4-dioxahexyl)-2,3-xylylene]-tetrahydro-3a,6a-diphenylimidazo[4,5-*d*]imidazole-2,5(1*H*,3*H*)-dione (6b). Under a nitrogen atmosphere the tetrahalide **6a** (1 g, 1 mmol) was mixed with a solution of sodium benzimidazolate (1.11 g, 8 mmol) in 25 mL of DMF and stirred for 16 h at 80 °C. DMF was evaporated in vacuo. Then, 20 mL of $CHCl_3$ was added. The organic layer was washed (10×) with 15 mL of acidic water (the pH was adjusted to 6 with concentrated HCl), dried ($MgSO_4$), and evaporated in vacuo: yield approximately 80% of **6b** as a white solid; mp >100 °C (dec); FABMS $(M + H)^+$ *m/e* 1315; IR (KBr) 1720 (C=O), 1130–1070 (COC) cm^{-1}; ^1H NMR ($CDCl_3$) δ 7.9–7.1 (br, 20 H, BenzH), 7.0 (s, 10 H, PhH), 6.3 (s, 4 H, XyH), 5.4 (d from AB q, 4 H, NC*H*H), 4.3–3.9 (br, 36 H, NCH*H* and $OCH_2CH_2OCH_2CH_2$). Anal. Calcd for $C_{76}H_{74}O_{10}N_{12}\cdot(H_2O)_{2.3}$: C, 67.21; H, 5.79; N, 12.38; O, 14.50. Found: C, 67.21; H, 5.91; N, 12.02; O, 14.86.

1,3:4,6-Bis[1,4-(9-chloro-1,4,7-trioxanonyl)-2,3-xylylene]tetrahydro-3a,6a-diphenylimidazo[4,5-*d*]imidazole-2,5(1*H*,3*H*)-dione (7a). This compound was prepared as described for **6a**. As an alkylating agent 1-tosyl-8-chloro-3,6-dioxaoctane was used. The resulting tetrachloride **7a** was a white gummy substance. Its ^1H NMR spectrum ($CDCl_3$) corresponds to that for **6a**, except for δ 3.8 (m, 52 H, NCH*H* and $(OCH_2CH_2)_2OCH_2CH_2Cl$).

1,3:4,6-Bis[1,4-(9-(1-benzimidazolyl)-1,4,7-trioxanonyl)-2,3-xylylene]tetrahydro-3a,6a-diphenylimidazo[4,5-*d*]imidazole-2,5(1*H*,3*H*)-dione (7b). This compound was prepared from **7a** and sodium benzimidazolate as described for **6b**. Podand **7b** has been obtained as a colorless syrup: yield ≈ 75% FABMS $(M + H)^+$ *m/e* 1491; IR (NaCl disks) 1720 (C=O), 1130–1070 (COC); ^1H NMR ($CDCl_3$) as for **7a** and **4** within 0.1 ppm. Anal. Calcd for $C_{84}H_{90}O_{14}N_{12}\cdot(H_2O)_{0.8}$: C, 66.91; H, 6.08; N, 11.15; O, 15.72. Found: C, 67.09; H, 6.42; N, 10.66; O, 15.83.

1,3:4,6-Bis[1,4-(4-(3-pyridyl)-1-oxabutyl)-2,3-xylylene]tetrahydro-3a,6a-diphenylimidazo[4,5-*d*]imidazole-2,5(1*H*,3*H*)-dione (8). Under a nitrogen atmosphere compound **5** (0.33 g, 0.6 mmol) was dissolved in 13.4 mL of DMSO containing K_2CO_3 (3.3 g, 24 mmol). Compound **10** (1 g, 3.6 mmol) was added, and the reaction mixture was stirred at 40 °C for 48 h. Thereafter, 40 mL of $CHCl_3$ was added, and the organic layer was washed (10×) with 50 mL of water. The chloroform layer was concentrated to about 2 mL and added dropwise, while stirring vigorously, to 100 mL of distilled ethyl acetate. After filtration the ethyl acetate layer was evaporated in vacuo, yielding 340 mg (55%) of **8**. The residue was dissolved in $CHCl_3$ and chromatographed over Sephadex LH-20, yielding another 120 mg (20%) of **8**: total yield 75% of light yellow solid 8; mp >100 °C (dec); FABMS $(M + H)^+$ *m/e* 1039; IR (KBr) 1720 (C=O) cm^{-1}; ^1H NMR ($CDCl_3$) δ 8.2 (s, 8 H, PyH), 7.3–6.5 (m, 18 H, PyH and PhH), 6.4 (s, 4 H, XyH), 5.5 (d from AB q, 4 H, NC*H*H, *J* = 16 Hz), 3.8 (m, 12 H, NCH*H* and OCH_2), 2.8 (m, 8 H, CH_2Py), 2.0 (m, 8 H, $OCH_2CH_2CH_2Py$). Anal. Calcd for $C_{64}H_{62}O_6N_8\cdot(H_2O)_{1.2}$: C, 72.41; H, 6.07; N, 10.56; O, 10.86. Found: C, 72.39; H, 6.33; N, 10.46; O, 10.83.

1,3:4,6-Bis[1,4-(8-(3-pyridyl)-1,4,7-trioxaoctyl)-2,3-xylylene]tetrahydro-3a,6a-diphenylimidazo[4,5-*d*]imidazole-2,5(1*H*,3*H*)-dione (9). Under a nitrogen atmosphere compound **5** (1.63 g, 3.0 mmol) was dissolved in 32.6 mL of DMSO containing powdered KOH (5.92 g, 0.11 mol). To this reaction mixture was added compound **11** (5 g, 23 mmol), and the mixture was stirred for 48 h at 65 °C. The mixture was poured into 150 mL of CH_2Cl_2 and washed (10×) with 100 mL of water. The organic layer was concentrated in vacuo and added dropwise, while stirring vigorously, to 300 mL of ethyl acetate. The precipitate was filtered off, and the solvent was evaporated in vacuo. The residue was dissolved in a minimum amount of methanol and chromatographed over Sephadex LH-20: yield 1.48 g (40%) of **9** as a yellow syrup; FABMS $(M + H)^+$ *m/e* 1279; IR (NaCl disks) 1720 (C=O), 1130–1070 (COC) cm^{-1}; ^1H NMR ($CDCl_3$) δ 8.4 (br, 8 H, PyH), 7.7–7.0 (m, 8 H, PyH), 6.9 (s, 10 H, PhH), 6.5 (s, 4 H, XyH), 5.5 (d from AB q, 4 H, NC*H*H, *J* = 16 Hz), 4.5 (s, 8 H, OCH_2Py), 3.8 (m, 36 H, NCH*H* $OCH_2CH_2OCH_2CH_2$). Anal. Calcd for $C_{72}H_{78}O_{14}N_8\cdot(H_2O)_{2.5}$: C, 65.28; H, 6.27; N, 8.46; O, 19.95. Found: C, 65.26; H, 6.23; N, 8.42; O, 20.09.

3-(3-Bromopropyl)pyridine Hydrogen Bromide (10·HBr). This compound was prepared according to a literature procedure.[25]

1-Chloro-7-(3-pyridyl)-3,6-dioxaheptane (11). Under a nitrogen atmosphere 3-pyridylcarbinol (2.07 g, 20 mmol) was dissolved in 25 mL of DMF. The solution was stirred and 1-tosyl-5-chloro-3-oxapentane (5.3 g, 20 mmol) was added, as well as powdered KOH (2 g, 35.7 mmol). This reaction mixture was stirred for 16 h. The KOH was filtered off, and 150 mL of CH_2Cl_2 was added. The resulting solution was washed with water (50 mL, 10×), dried ($MgSO_4$), and evaporated in vacuo: yield 2.37 g (55%) of **11** as a yellow oil; ^1H NMR ($CDCl_3$) δ 8.4 (m, br, 2 H, PyH), 7.8–7.0 (m, br, 2 H, PyH), 4.5 (s, 2 H, OCH_2Py), 3.6 (s, 8 H, $OCH_2CH_2OCH_2CH_2Cl$).

***trans*-[Rh(2a)Cl$_2$]Cl.** $RhCl_3\cdot 3H_2O$ (26.4 mg, 0.1 mmol) was dissolved in 50 mL of methanol and added instantaneously, while stirring vigorously, to a solution of the tetrapodand **2** (96.6 mg, 0.1 mmol) in 50 mL of methanol. The mixture was stirred for 48 h, filtered over infusorial earth, and concentrated in vacuo: yield 67.0 mg (57%) of the glassy yellow compound *trans*-[Rh(**2a**)Cl_2]Cl; mp >200 °C; FABMS $(M - Cl)^+$ *m/e* 1139; IR (KBr) 1720 (C=O), (transreflection) 344 (RhCl); ^1H NMR (CD_3OD) δ 8.25 (pseudo s, 4H, NCHN), 7.40 (s, br, 4H, N(1)C*H*CHN(3)), 7.20–6.90 (m, 14 H, ArH and N(1)CHC*H*N(3)), 4.85 (AB q, J_{gem} = 12 Hz, 8 H, NCH_2O), 4.30 (t, AA′BB′, 8 H, CH_2Im), 3.60 (m, 16 H, OCH_2CH_2O). Anal. Calcd for $C_{48}H_{62}N_{12}O_{10}Cl_3Rh\cdot(H_2O)_{6.4}$: C, 44.63; H, 5.80; N, 13.02; O, 20.33. Found: C, 44.18; H, 5.71; N, 13.39; O, 20.75.

***trans*-[Rh(2b)Cl$_2$]Cl.** This compound was prepared by the same route as *trans*-[Rh(**2a**)Cl_2]Cl: yield 34% of the glassy light yellow compound *trans*-[Rh(**2b**)Cl_2]Cl; mp >200 °C (dec); FABMS $(M - 2Cl)^+$ *m/e* 928; IR (KBr) 1720 (C=O) cm^{-1}; ^1H NMR (CD_3OD) δ 8.1 (s, 4 H, NCHN), 7.3–6.5 (m, 18 H, ArH and NCHCHN), 4.65 (AB q, J_{gem} = 12 Hz, 8 H, NCH_2O), 4.4 (m, 8 H, CH_2Im), 4.75 (m, 8 H, OCH_2). The elemental analysis of this compound is not reproducible.

***ex-cis*-[Rh(3)Cl$_2$]Cl.** This compound was prepared as described for *trans*-[Rh(**2a**)Cl_2]Cl: yield 52% of the glassy yellow compound *ex-cis*-[Rh(**3**)Cl_2]Cl; mp >200 °C (dec); FABMS $(M - Cl)^+$ *m/e* 1315; IR

(24) Butler, A. R.; Leitch, E. *J. Chem. Soc., Perkin Trans. 2* **1980**, 103–109.

(25) Beeby, P. J.; Sandheimer, F. *J. Am. Chem. Soc.* **1972**, *94*, 2128.

Table III. FABMS Results of *trans*-[Rh(**6b**)Cl_2)]Cl

m/e	relative intensity, %	assgnt
1315	100	$(M - 3Cl - Rh + H)^+$
1415	17	$(M - 3Cl - 2H)^+$
1452	41	$(M - 2Cl)^+$
1487	49	$(M - Cl)^+$
1475	10	$(M - 2Cl + NBA^a - NO)^+$
1605	8	$(M - 2Cl + NBA)^+$

[a] NBA = *m*-nitrobenzyl alcohol.

(KBr) 1720 (C=O), (transreflection) 338 (RhCl); ^1H NMR (CD_3OD) δ 8.5–7.8 (br, 4 H, NCHN), 7.5–6.7 (br, 18 H, ArH and NCHCHN), 5.1–4.5 (br, 8 H, NCH_2O), 4.3 (t, br, 8 H, CH_2Im), 4.0–3.3 (m, 40 H, $O(CH_2CH_2O)_2CH_2$).

***trans*-[Rh(4)Cl_2]Cl.** $RhCl_3 \cdot 3H_2O$ (26.4 mg, 0.1 mmol) was dissolved in 50 mL of methanol and added instantaneously, while stirring vigorously, to a hot solution of tetrapodand **4** (134.2 mg, 0.1 mmol). The mixture was refluxed for 16 h, filtered over infusorial earth, and evaporated in vacuo: yield 121 mg (78 %) of the glassy yellow compound *trans*-[Rh(**4**)Cl_2]Cl; mp >200 °C (dec); FABMS $(M - Cl)^+$ *m/e* 1515; ^1H NMR ($CDCl_3$) δ 8.2 (br, 4 H, NCHN), 7.8–6.4 (m, br, 26 H, ArH and BenzH), 4.9–4.1 (br, 16 H, NCH_2O and CH_2Benz), 4.0–3.1 (br, 40 H, $O(CH_2CH_2O)_2CH_2$). Anal. Calcd for $C_{72}H_{86}N_{12}O_{14}RhCl_3 \cdot (H_2O)_4$: C, 53.17; H, 5.78; N, 10.34; O, 17.72. Found: C, 53.28; H, 5.88; N, 10.20; O, 17.72.

***trans*-[Rh(6b)Cl_2]Cl. Procedure 1.** This compound was synthesized from $RhCl_3 \cdot 3H_2O$ and **6b** as described for *trans*-[Rh(**4**)Cl_2]Cl: mp >170 °C (dec); FABMS $(M - Cl)^+$ *m/e* 1487. The FAB mass spectrum of *trans*-[Rh(**6b**)Cl_2)]Cl displays not only an intense isotope pattern belonging to the Rh-containing molecular ion $(M - Cl)^+$ *m/e* 1487 but, in addition, signal patterns at *m/e* 1575 and 1605. The isotope distribution for both patterns is similar to the one for $(M - 2Cl)^+$. The difference in mass numbers between *m/e* 1605 and 1452 (for $(M - 2Cl)^+$) is exactly the mass of a matrix molecule *m*-nitrobenzyl alcohol (see Table III). Furthermore, the signal at *m/e* 1575 can be assigned to $(M - 2Cl)^+$ plus *m*-nitrobenzyl alcohol minus an NO fragment. Apparently, *trans*-[Rh(**6b**)Cl_2)]Cl forms a host–guest type adduct with a matrix molecule: ^1H NMR ($CDCl_3$) δ 8.5–7.2 (br, 20 H, BenzH), 7.0 (s, 10 H, PhH), 6.8–6.1 (br, 4 H, XyH), 5.9–5.1 (br, 4 H, NC*H*H), 4.8–3.1 (br, 36 H, NCH*H* and $OCH_2CH_2OCH_2CH_2$); IR (KBr) 1720 (C=O); 1110–1060 (COC) cm^{-1}. Anal. Calcd for $C_{76}H_{74}O_{10}N_{12}Cl_3Rh \cdot (H_2O)_{12}$: C, 52.39; H, 5.63; N, 9.65; O, 20.22. Found: C, 52.51; H, 6.51; N, 8.41; O, 20.76. The compound is very hygroscopic and rapidly becomes inhomogeneous; consequently, elemental analysis is difficult to perform.

***trans*-[Rh(6b)Cl_2]Cl. Procedure 2. DMSO/EtOH Reaction.**[22] Under a nitrogen atmosphere **6b** (100 mg, 0.076 mmol) was dissolved in a mixture of 38 mL of DMSO and 38 mL of ethanol. To this reaction mixture was added $RhCl_3 \cdot 3H_2O$ (20 mg, 0.076 mmol). The solution was stirred and heated to 100 °C for 2 h. DMSO and ethanol were evaporated in vacuo, yielding the complex as a yellow solid in quantitative yield.

***trans*-[Rh(6b)Cl_2]Cl. Procedure 3. DMSO/H_2 Reaction.**[23] Under a nitrogen atmosphere **6b** (50 mg, 0.038 mmol) was dissolved in 38 mL of DMSO. To this reaction mixture was added $RhCl_3 \cdot 3H_2O$ (10 mg, 0.038 mmol). The reaction mixture was stirred and molecular hydrogen was bubbled through the solution for 10 h at 20 °C. DMSO was evaporated in vacuo, yielding the complex as a yellow solid in quantitative yield.

***trans*-[Rh(7b)Cl_2]Cl.** This compound was synthesized from $RhCl_3 \cdot 3H_2O$ and **7b** as described for *trans*-[Rh(**4**)Cl_2]Cl: mp >245 °C (dec); FABMS $(M - Cl)^+$ *m/e* 1663; ^1H NMR ($CDCl_3$) δ 8.5–7.1 (br, 20 H, BenzH), 6.9 (s, 10 H, PhH), 5.9–5.1 (br, 4 H, NC*H*H), 4.7–2.8 (br, 52 H, NCH*H* and $OCH_2CH_2OCH_2CH_2OCH_2CH_2$); IR (KBr) 1720 (C=O); 1110–1060 (COC) cm^{-1}. Anal. Calcd for $C_{84}H_{90}N_{12}O_{14}Cl_3Rh \cdot (H_2O)_7$: C, 55.17; H, 5.69; N, 9.20; O, 18.39. Found: C, 55.33; H, 5.80; N, 9.03; O, 17.90.

***trans*-[Rh(8)Cl_2]Cl.** This compound was synthesized from $RhCl_3 \cdot 3H_2O$ and **8** as described for *trans*-[Rh(**4**)Cl_2]Cl: mp >200 °C (dec); FABMS $(M - Cl)^+$ *m/e* 1211; ^1H NMR ($CDCl_3$) δ 8.9–6.0 (br, 20 H, PyH and PhH), 7.0 (s, 10 H, PhH), 5.6 (br, 4 H, NC*H*H), 4.1–3.2 (br, 12 H, NCH*H* and $OCH_2CH_2CH_2$), 3.2–2.4 (br, 8 H, $OCH_2CH_2CH_2$), 2.2–1.7 (br, 8 H, $OCH_2CH_2CH_2$); IR (KBr) 1720 (C=O). Anal. Calcd for $C_{64}H_{62}O_6N_8Cl_3Rh \cdot (CH_3OH) \cdot (H_2O)_4$: C, 57.67; H, 5.77; N, 8.28; O, 13.01. Found: C, 57.79; H, 5.54; N, 7.94; O, 12.79.

***trans*-[Rh(9)Cl_2]Cl.** This compound was synthesized from $RhCl_3 \cdot 3H_2O$ and **9** as described for *trans*-[Rh(**4**)Cl_2]Cl: mp >180 °C (dec); FABMS $(M - Cl)^+$ *m/e* 1451; ^1H NMR (CD_3OD) δ 8.8–6.0 (br, 30 H, PyH, PhH), 5.8–5.1 (br, 4 H, NC*H*H), 4.9–3.0 (br, 36 H, NCH*H* and $(OCH_2CH_2)_2$). Anal. Calcd for $C_{72}H_{78}N_8O_{14}Cl_3Rh \cdot (H_2O)_6$: C, 54.11; H, 5.64; N, 7.01; O, 20.04. Found: C, 54.08; H, 5.65; N, 6.89; O, 19.85.

***trans*-[Rh(11)$_4$$Cl_2$]Cl.** Under a nitrogen atmosphere compound **11** (86.9 mg, 0.4 mmol) was dissolved in 100 mL of methanol. To this mixture was added $RhCl_3 \cdot 3H_2O$ (26.6 mg, 0.1 mmol). The reaction mixture was refluxed for 2 h. Thereafter, the methanol was evaporated in vacuo, yielding the complex as a yellow oil in quantitative yield: FABMS $(M - Cl)^+$ *m/e* 1035; ^1H NMR (CD_3OD) δ 8.75–6.95 (m, 16 H, PyH), 4.5 (s, 8 H, OCH_2Py), 3.55 (m, 32 H, $ClCH_2CH_2OCH_2CH_2$). Anal. Calcd for $C_{40}H_{56}O_8N_4Cl_7Rh \cdot (H_2O)_2$: C, 43.32; H, 5.42; N, 5.05; O, 14.44. Found: C, 43.18; H, 5.48; N, 4.86; O, 14.77.

***trans*-[Rh(12)$_4$$Cl_2$]Cl.** Under a nitrogen atmosphere compound **12** (66 mg, 0.5 mmol) was dissolved in 100 mL of methanol. To this mixture was added $RhCl_3 \cdot 3H_2O$ (32.9 mg, 0.125 mmol). The reaction mixture was refluxed for 2 h. Subsequently, the methanol was evaporated in vacuo, yielding the complex as a yellow solid in quantitative yield: mp >230 °C; FABMS $(M - Cl)^+$ *m/e* 703; ^1H NMR ($CDCl_3$) δ 8.2–6.3 (br, 20 H, BenzH), 4.4–3.2 (br, 12 H, CH_3). Anal. Calcd for $C_{32}H_{32}N_8Cl_3Rh \cdot (CH_3OH) \cdot (H_2O)_4$: C, 47.03; H, 5.23; N, 13.30. Found: C, 46.89; H, 5.02; N, 13.13.

Acknowledgment. Dr. D. M. Grove and Professor W. Dreuth are kindly thanked for their discussions and helpful advice during the preparation of the manuscript.

Registry No. 1, 101241-21-8; **3**, 118715-66-5; **4**, 118722-46-6; **5**, 106319-02-2; **6a**, 118715-67-6; **6b**, 118715-68-7; **7a**, 118715-69-8; **7b**, 118715-70-1; **8**, 118715-71-2; **9**, 118715-72-3; **10**·HBr, 41038-63-5; **11**, 118715-73-4; *trans*-[Rh(**2a**)Cl_2]Cl, 101333-07-7; *trans*-[Rh(**2b**)Cl_2]Cl, 118715-76-7; *ex-cis*-[Rh(**3**)Cl_2]Cl, 118715-77-8; *trans*-[Rh(**4**)Cl_2]Cl, 118715-78-9; *trans*-[Rh(**6b**)Cl_2]Cl, 106319-07-7; *trans*-[Rh(**7b**)Cl_2]Cl, 118715-79-0; *trans*-[Rh(**8**)Cl_2]Cl, 118715-80-3; *trans*-[Rh(**9**)Cl_2]Cl, 118715-81-4; *trans*-[Rh(**11**)$_4$$Cl_2$]Cl, 118715-82-5; *trans*-[Rh(**12**)$_4$$Cl_2$]Cl, 118715-83-6; 1-chloro-8-hydroxy-3,6-dioxaoctane, 5197-62-6; sodium imidazolate, 5587-42-8; 1-tosyl-5-chloro-3-oxapentane, 118715-74-5; sodium benzimidazolate, 1073-32-1; 1-tosyl-8-chloro-3,6-dioxaoctane, 118715-75-6.